

# Structure of nitrogen molecular clusters $(\text{N}_2)_n$ with $13 \leq n \leq 55$

 F. Calvo<sup>1,a</sup>, A. Boutin<sup>2</sup>, and P. Labastie<sup>1</sup>
<sup>1</sup>Laboratoire Collisions, Agrégats, Réactivité (UMR 5589, CNRS) IRSAMC, Université Paul Sabatier, 118 Route de Narbonne, F-31062 Toulouse Cédex, France

<sup>2</sup>Laboratoire de Chimie-Physique des Matériaux Amorphes, Department of Physical Chemistry, Bâtiment 490, Université Paris-Sud, F-91405 Orsay Cédex, France

Received: 2 September 1998 / Received in final form: 28 September 1998

**Abstract.** We investigate the structural properties of nitrogen molecular clusters  $(\text{N}_2)_n$  using classical Monte Carlo simulations and optimization methods. As is the case for argon clusters, we find polyicosahedral (anti-Mackay) geometries above 13 molecules, and multilayer icosahedra with uncomplete outer shell (Mackay) geometries below 55 molecules. The crossover point between these two kinds of structures is located near 42 molecules, whereas it is at only 31 for argon. With a simple three-body (Axilrod–Teller) potential added to the standard Lennard–Jones model, we interpret this difference as the result of the strong anisotropy of the molecular potential.

**PACS.** 36.40.Mr Spectroscopy and geometrical structure of clusters

## 1 Introduction

Over the past decade, simple atomic clusters bound by the common Lennard–Jones (LJ) or Morse potentials have been extensively studied for their static and dynamical properties. They have also provided prototype models for testing methodology in areas such as global optimization [1, 2] or for carrying out numerical calculations of thermodynamical quantities [3, 4]. More complex species, especially metallic clusters [5], could then be efficiently investigated by the use of the techniques developed on these simple systems.

By comparison, molecular systems have been given much less attention, perhaps with the exception of water [6]. Van der Waals molecular clusters are probably the most simple to model and describe. With the increasing computational power available, it has become possible to undertake studies for molecular clusters that are similar to those done on atomic clusters and in which the clusters are in the same size range (up to about a few hundred molecules).

For instance, the crystalline crossover size could be properly determined for both sulfur hexafluoride [7] and carbon dioxide [8] through the use of computer simulations as well as experiments. Below this size, van der Waals clusters usually exhibit size-dependent shapes, often with pentagonal symmetry and icosahedral units. Larger clusters tend to adopt a more pronounced face-centered cubic (FCC) character, which leads to bulk matter. While the

crystalline crossover point is estimated in the range 1000–2000 for argon [9], it is only  $\sim 15$  for  $\text{SF}_6$  [7] and  $\sim 30$  for  $\text{CO}_2$  [8]. These differences between atomic and molecular van der Waals clusters were attributed to the strong anisotropy of the intermolecular potentials [10].

A recent theoretical estimation [11] based upon a model by Doye *et al.* [12] and the experimental results of Torchet and De Feraudy [13] have both predicted the crystalline crossover size to be located near 100–200 molecules for nitrogen molecular clusters. At the present time, no direct comparison with simulation has been made to check and specify this value, and the relatively large critical size makes extensive numerical studies harder to undertake than they have been for carbon dioxide. However, smaller nitrogen clusters remain interesting in many aspects. Up to the size  $n = 13$ , the structures formed by the molecular centers of mass in  $(\text{N}_2)_n$  free clusters are the same as the atoms' locations in simpler  $\text{LJ}_n$  clusters [14, 15], whereas some differences seem to appear in the vapor phase [16]. In other terms, there is a general isomorphism between the preferred geometries of  $\text{LJ}_n$  and the centers of mass in  $(\text{N}_2)_n$ . In this paper, we investigate the structure of  $(\text{N}_2)_n$  clusters in the size range  $13 \leq n \leq 55$ , by means of simulations and numerical methods. In this size range, a crossover between polyicosahedral and multilayer icosahedral structures occurs. We seek to answer the question: How is such a crossover displaced by the molecular character of the clusters?

This paper is organized as follows. In Sect. 2 we briefly describe the potential chosen to model the interaction between  $\text{N}_2$  molecules, and the methodology used through-

---

<sup>a</sup> e-mail: florent@yosemite.ups-tlse.fr

out. The structures found are presented in Sect. 3, and the results are interpreted with a simple anisotropic atomic model. We finally summarize and conclude in Sect. 4.

## 2 Methods

The potential used to model the interaction between  $N_2$  molecules has been widely employed in previous studies on bulk [17] and clusters [11, 18, 19]. The molecules are considered to be rigid, and the interaction between them is modeled by four partial Coulombic charges located on the N–N bond, plus a repulsion-dispersion term of the Buckingham form on the nitrogen atoms. Four global optimization methods were used to find the lowest structures of  $(N_2)_n$  clusters,  $13 \leq n \leq 55$ . First, a standard Monte Carlo simulated annealing (MCSA) was performed from randomly placed and oriented molecules inside a cubic box. A steepest descent quenching procedure with adaptive stepsize ended the MCSA searches. Regular quenching along a high-temperature MC trajectory also provided bunches of structures lying low in energy. A Monte Carlo growth algorithm was used, in a similar way as in [14]. Finally, we also used a slightly modified version of the basin-hopping method of Wales and Doye [1].

Up to now, this “basin-hopping” method has been the most successful in finding the absolute minima of  $LJ_n$  clusters up to size 110, including pathological structures such as  $LJ_{38}$  (truncated octahedral) or  $LJ_{75}$  (decahedral). More recently, it has also been applied to Sutton–Chen clusters [20]. Its basic principle is that a Monte Carlo simulation is performed on the deformed and discontinuous potential-energy surface (PES)  $\tilde{V}(\mathbf{R})$  obtained by quenching from configuration  $\mathbf{R}$ . In the original method [1], all atoms are initially randomly placed inside a cubic box. After each quench, collective random displacements of all atoms are followed by another quench leading to the next possible configuration, accepted with the Metropolis probability. In order to more easily find several structures close in geometry and/or in energy, we chose to displace only a subset of the whole cluster. Every 500 quenches, we regularly decreased the number  $n^*$  of molecules to be moved ( $n^*$  becoming  $n^* - 2$ ). A total of 5000 quenches were performed for each simulation at a given size, starting with  $n^* = n$ .

After a good candidate for the global minimum was found by one of the methods described above, we carried out a series of regular quenches along an MC trajectory at  $T = 25$  K to further optimize the molecular orientations, since orientational disorder prevails at this temperature [18].

## 3 Structures of $(N_2)_n$ clusters, $13 \leq n \leq 55$

The lowest energies of the structures found by the various algorithms described above for the  $(N_2)_n$  clusters are plotted in Fig. 1 *versus* the molecular size  $n$ . The main result is

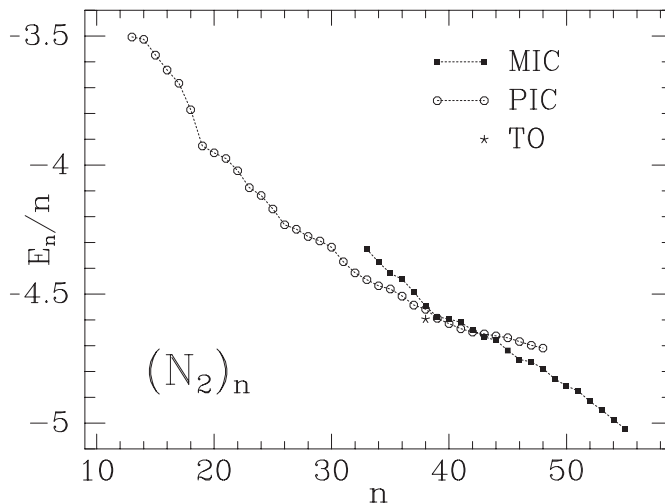


**Fig. 1.** Energies of the lowest structures of  $(N_2)_n$  clusters. The three different kinds of arrangements found for the molecular centers of mass are polyicosahedral (PIC, open circles), multi-layer icosahedral (MIC, full squares), and truncated octahedral (TO, star).  $E_n/n$  is in  $\text{kJ mol}^{-1}\text{molecule}^{-1}$ .

the classification of most structures between the two categories already known for argon clusters [21], namely polyicosahedral (PIC, or anti-Mackay) and multilayer icosahedral with uncomplete external layer (MIC, or Mackay). In both categories, one considers the growth of clusters from the perfect icosahedron ( $n = 13$ ) by adding atoms either over the center of triangular facets (anti-Mackay construction), or on the edges of these facets. This latter construction leads to the perfect Mackay icosahedron at  $n = 55$ . Just above the simple icosahedron made of 13 molecules, the clusters tend to maximize the number of nearest-neighbor bonds between molecules. The resulting anti-Mackay construction is illustrated in Fig. 2(a) on the example of  $(N_2)_{34}$ . As the number of external molecules increases, the stress exerted by these molecules on the inner part of the cluster also increases. On the other hand, the Mackay construction is less local, and favors the building of larger sizes by entire planes. The inner molecules are much less constrained, and the number of nearest neighbors is smaller than in the polyicosahedra.  $(N_2)_{49}$ , in its lowest-energy configuration, has a Mackay-type geometry represented in Fig. 2(b).

The perfect Mackay icosahedra are well-known magic numbers in argon clusters. By adding capped pentagonal rings over the primitive icosahedron, one creates clusters made of intertwined double icosahedron units [22]. The extra stability of these geometries is reflected in the secondary magic numbers 19, 23, 26, 29, 32, and 34 seen by Harris and his coworkers in mass spectra experiments on argon microclusters [23]. Similarly, missing facets on the external layer of the  $n = 55$  icosahedron lead to another series of secondary magic numbers, 49, 46, 43, and 39, also seen by Harris *et al.* [23]. In Fig. 3, we have calculated the relative energetic stability  $\Delta_2 E(n) = E_{n+1} + E_{n-1} - 2E_n$  as a function of the size  $n$ . Indeed, both series can be seen in Fig. 3. However, the numbers 32 and 34

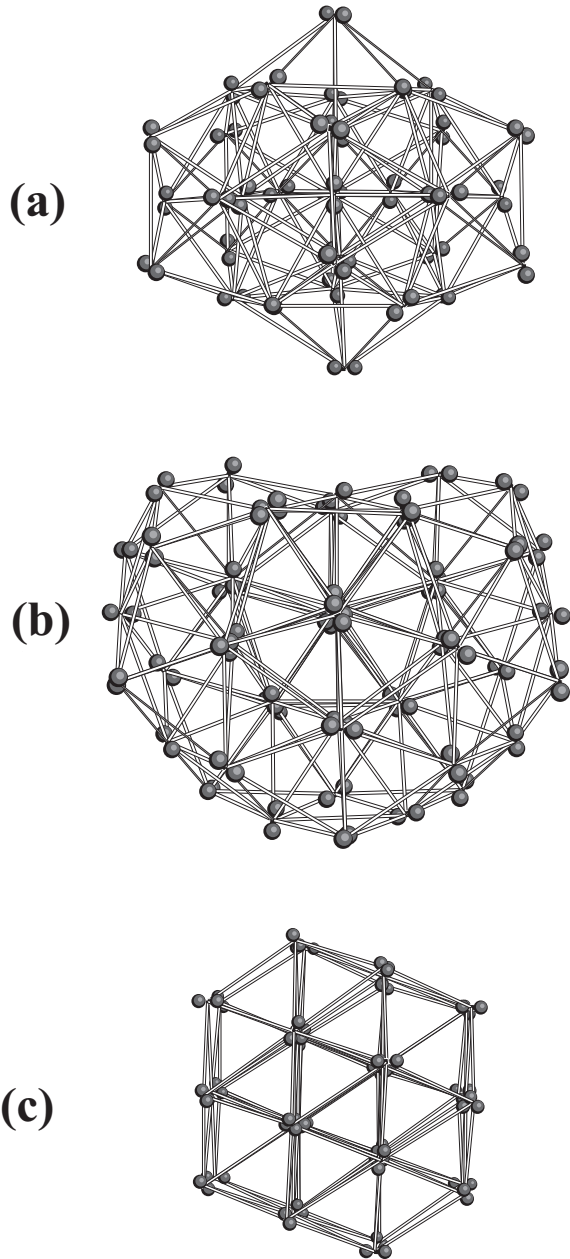


**Fig. 2.** Lowest-energy structures of selected  $(\text{N}_2)_n$  clusters. (a)  $(\text{N}_2)_{34}$ ,  $E = -4.467 \text{ kJ mol}^{-1} \text{ molecule}^{-1}$  (anti-Mackay); (b)  $(\text{N}_2)_{49}$ ,  $E = -4.829 \text{ kJ mol}^{-1} \text{ molecule}^{-1}$  (Mackay); (c)  $(\text{N}_2)_{38}$ ,  $E = -4.597 \text{ kJ mol}^{-1} \text{ molecule}^{-1}$  (truncated octahedron).

are poorly marked for argon, whereas the numbers 39 and 43 are poorly marked for nitrogen. This is consistent with the difference in crossover size between anti-Mackay and Mackay geometries, which is only 31 for argon [21], and 42 for nitrogen in Fig. 1.

One important similarity between argon and nitrogen in the size range  $13 \leq n \leq 55$  is the discovery of a very peculiar structure for  $n = 38$ , a truncated octahedron, initially found by Doye *et al.* [12] and independently by Pillardy and Piela [24] in LJ systems. This cluster appears

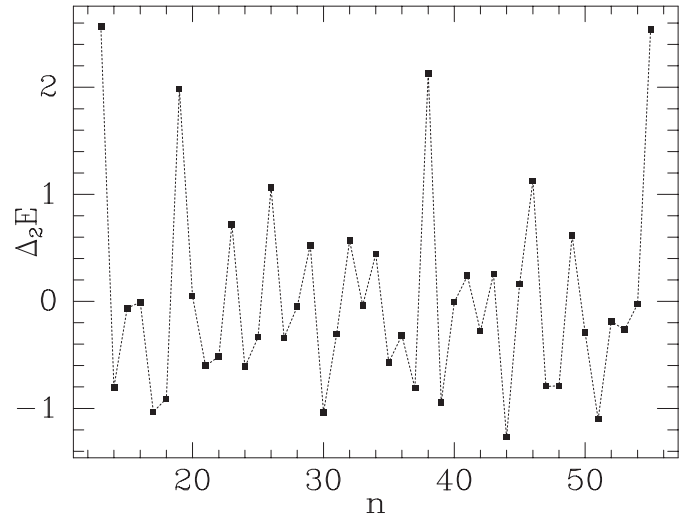


**Fig. 3.** Relative energetic stability  $\Delta_2 E(n)$  versus the size  $n$  for  $(\text{N}_2)_n$  clusters in their global minimum.  $\Delta_2 E$  is in  $\text{kJ mol}^{-1}$ .

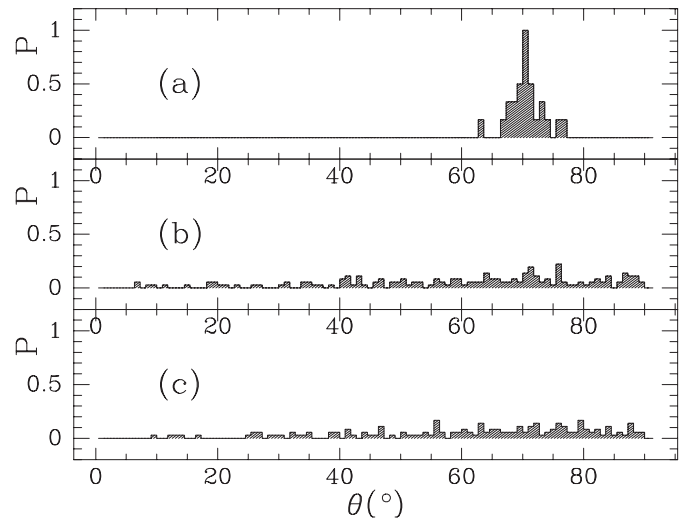


**Fig. 4.** Unnormalized probabilities of observing the angle  $\theta$  between the relative orientations of nearest-neighbor molecules in  $(\text{N}_2)_{38}$  at  $T = 0 \text{ K}$  and in different geometries. (a) Truncated octahedral shape; (b) polyicosahedral shape; (c) multi-layer icosahedral shape.

as a nearly perfect subpart of the bulk FCC molecular nitrogen, and is represented in Fig. 2(c). As a consequence, the relative orientations of the molecules are very different in  $(\text{N}_2)_{38}$  in its ground state (at 0 K) and in its polyicosahedral and multilayer icosahedral shapes. Figure 4 shows the spectra of these relative orientations between nearest-neighbor molecules. While the spectra are rather broad for the PIC and MIC structures, the spectrum for the truncated octahedron is much sharper and centered at the bulk limit  $\theta_{\text{bulk}} = \arccos 1/3 \simeq 70^\circ 30'$ . The present results show that the qualitative isomorphism observed by Bertolus *et al.* between molecular nitrogen and argon clusters below 13 molecules [14] remains valid up to the next Mackay shell, including the special case  $n = 38$ . There are

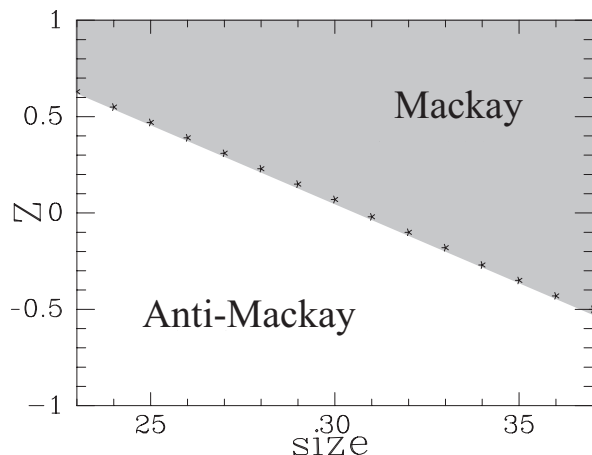


**Fig. 5.** Relative stabilities of anti-Mackay and Mackay structures *versus* the size  $n$  and the magnitude  $Z$  of the Axilrod–Teller anisotropy in the Lennard–Jones model.

nevertheless some differences: The tendency towards formation of anti-Mackay structures is stronger for nitrogen, and the crossover size is significantly larger. We propose now an interpretation of these differences with a simple atomic model.

To the standard LJ potential, we add the three-body anisotropic contribution of the Axilrod–Teller potential:

$$V_{\text{AT}}(\mathbf{R}) = Z \sum_{i < j < k} \frac{1 + 3 \cos \theta_1 \cos \theta_2 \cos \theta_3}{(r_{ij} r_{jk} r_{ik})^3} \quad (1)$$

The effects of such a perturbation on the structure and PES topography of  $\text{LJ}_n$  clusters was previously investigated by Wales [25]. The magnitude  $Z$  of the anisotropy is treated as a free parameter inside the range  $-1 \leq Z \leq 1$ . Depending on the sign of  $Z$ , a structure can either be further stabilized with respect to another, or the opposite. As shown by Wales [25], negative values of  $Z$  favor compact geometries with many triangular facets between nearest neighbors. In contrast, positive values of  $Z$  favor open geometries. Since polyicosahedra have more nearest-neighbor interactions (especially on surface) than multilayer icosahedra, one can expect a strong effect of the Axilrod–Teller term on the relative stability of PIC and MIC arrangements. We have locally optimized the structure of  $\text{LJ}_n$  clusters perturbed by this anisotropic potential, in the range  $27 \leq n \leq 37$ , for both anti-Mackay and Mackay geometries. The resulting stability diagram is represented in Fig. 5. The crossover size between PIC and MIC geometries linearly increases from 27 at  $Z \sim 0.63$  to 37 at  $Z \sim -0.51$ , which is in agreement with Wales’ results [25]. Hence the anisotropy of the potential can be responsible for the large differences in this crossover point observed between argon and molecular nitrogen. In particular, as shown in Fig. 5, the sign of the three-body anisotropic contribution of the intermolecular potential for  $\text{N}_2$  should be negative. This result is also supported by the fact that, in the trimer  $(\text{N}_2)_3$ , one bond length is notably smaller than the other two (in length order: 3.73 Å, 4.11 Å and 4.12 Å).

Obviously the multicenter potential used in this study cannot be reduced to the simple Axilrod–Teller three-body potential. However, it contains some features, such as its intrinsic anisotropy, which can be modeled (in a first approach) by a development in  $N$ -body terms, the largest in magnitude being probably the Axilrod–Teller term. Focusing on the Axilrod–Teller potential as the single cause for anisotropy must not obscure our main result in this section, namely that the potential anisotropy should be responsible for the quantitative structural differences between argon and molecular nitrogen, and this despite large similarities and a global isomorphism in the range from 13 to 55 molecules.

Before concluding, we also wish to make a few comments on the efficiency of the global optimization methods we have used. Only the basin-hopping method of Wales and Doye [1] could find all the known lowest-energy structures in the whole range  $13 \leq n \leq 55$ , including  $n = 38$ . All other methods used in this study were unable to find the truncated octahedron at  $n = 38$ . The Monte Carlo growth method could even not find any MIC structure, because of the strong rearrangement required from the PIC geometry. Hence our results confirm the power of the basin-hopping algorithm, for which the only efficient competitors at the present time seem to be the genetic algorithms [2].

## 4 Conclusion

The structural properties of nitrogen molecular clusters  $(\text{N}_2)_n$  share many features, but also some differences, with the properties of simpler  $\text{LJ}_n$  atomic clusters in the range  $13 \leq n \leq 55$ . The same three kinds of arrangements are found for the molecular centers of mass as in the LJ case: polyicosahedral (also known as anti-Mackay) above 13 molecules, multilayer icosahedral with uncomplete outer layer (Mackay) below 55 molecules, and truncated octahedral for  $n = 38$ . The perfect Mackay icosahedra ( $n = 13$  and  $n = 55$ ) appear to be the most stable with respect to their neighboring sizes. Besides these two magic numbers, secondary magic sizes are found either when polyicosahedral clusters are entirely made of double icosahedron units ( $n = 19, 23, 26, 29, 32$ , and  $34$ ) or when there are complete facets missing from the external layer of the second Mackay icosahedron ( $n = 46$  and  $49$ ). These strong similarities of shape suggest that many intriguing thermodynamical effects seen in LJ clusters [26–29] could also exist in  $\text{N}_2$  clusters, especially dynamical coexistence [30].

The crossover size between polyicosahedra and multilayer icosahedra is located near 42  $\text{N}_2$  molecules, whereas it is at only 31 for LJ atomic clusters. To explain this difference, we have investigated the effects of an anisotropic three-body term added to the LJ potential on the relative stability of the Mackay and anti-Mackay constructions. We have found that the value of the corresponding crossover point is indeed very sensitive to the magnitude  $Z$  of this perturbative potential. Thus the natural anisotropy of the molecular potential is probably responsible for the larger crossover size. Furthermore, our study tends to show that

the three-body anisotropic contribution should be negative, as is the case for water [31]. This latter result still demands full *ab initio* calculations for verification, at least on the smaller systems.

Another important question still open concerns the crystalline crossover point from icosahedral to cubic geometries. Further investigations in the range 100–200 molecules are currently underway in order to determine its value.

The authors wish to thank G. Torchet for useful discussions. Support by the CNRS, the Région Midi-Pyrénées, the Université Paul Sabatier, and the MENRT is gratefully acknowledged.

## References

1. D.J. Wales, J.P.K. Doye: *J. Phys. Chem. A* **101**, 5111 (1997)
2. J.A. Niesse, H.R. Mayne: *J. Chem. Phys.* **105**, 4700 (1996)
3. J.P.K. Doye, D.J. Wales: *J. Chem. Phys.* **102**, 9659 (1995)
4. P. Labastie, R.L. Whetten: *Phys. Rev. Lett.* **65**, 1567 (1990)
5. F. Calvo, F. Spiegelmann: *Phys. Rev. B* **54**, 10 949 (1996)
6. K. Liu, J.D. Cruzan, R.J. Saykally: *Science* **271**, 929 (1996)
7. A. Boutin, J.-B. Maillet, A.H. Fuchs: *J. Chem. Phys.* **99**, 9944 (1993)
8. G. Torchet, M.-F. De Feraudy, A. Boutin, A.H. Fuchs: *J. Chem. Phys.* **105**, 3671 (1996)
9. S. Goyal, D.L. Schutt, G. Scoles: *J. Chem. Phys.* **102**, 2302 (1995)
10. A. Boutin, B. Rousseau, A.H. Fuchs: *Chem. Phys. Lett.* **218**, 122 (1994)
11. J.-B. Maillet, A. Boutin, S. Buttefey, F. Calvo: A.H. Fuchs: *J. Chem. Phys.* **109**, 329 (1998)
12. J.P.K. Doye, D.J. Wales, R.S. Berry: *J. Chem. Phys.* **103**, 4234 (1995)
13. F. Calvo, G. Torchet, M.-F. De Feraudy: *J. Chem. Phys.* (to be published)
14. M. Bertolus, V. Brenner, P. Millié, J.-B. Maillet: *Z. Phys. D* **39**, 239 (1997)
15. The ordering between the two lowest isomers is, however, reversed for  $(N_2)_8$  and  $LJ_8$
16. I. Rodríguez, A.J. Acevedo, G.E. López: *Mol. Phys.* **90**, 943 (1997)
17. H.-J. Böhm, R. Ahlrichs: *Mol. Phys.* **55**, 1159 (1985)
18. J.-B. Maillet, A. Boutin, A.H. Fuchs: *Phys. Rev. Lett.* **76**, 4336 (1996)
19. F. Calvo: *Phys. Rev. E* **58**, 5643 (1998)
20. J.P.K. Doye, D.J. Wales: *New J. Chem.* **22**, 733 (1998)
21. J.A. Northby: *J. Chem. Phys.* **87**, 6166 (1987)
22. J. Farges, M.-F. De Feraudy, B. Raoult, G. Torchet: *Surf. Sci.* **156**, 370 (1985)
23. I.A. Harris, R.S. Kidwell, J.A. Northby: *Phys. Rev. Lett.* **53**, 2390 (1984)
24. J. Pillardy, L. Piela: *J. Phys. Chem.* **99**, 11 805 (1995)
25. D.J. Wales: *J. Am. Chem. Soc. Faraday Trans.* **86**, 3505 (1990)
26. F. Calvo: *J. Chem. Phys.* **108**, 6861 (1998)
27. J.P.K. Doye, D.J. Wales: *Phys. Rev. Lett.* **80**, 1357 (1998); J.P.K. Doye, D.J. Wales, M.A. Miller: *J. Chem. Phys.* **109**, 8143 (1998)
28. F. Calvo, P. Labastie: *Chem. Phys. Lett.* **248**, 233 (1996)
29. H.-P. Cheng, R.S. Berry: *Phys. Rev. A* **45**, 7969 (1992)
30. D.J. Wales: *Mol. Phys.* **78**, 151 (1993)
31. C.S. Ewig: *J. Chem. Phys.* **92**, 6620 (1990)